THE JOURNAL OF BIOLOGICAL CHEMISTRY VOL. 290, NO. 42, pp. 25548–25560, October 16, 2015

Novel Regulation of the Synthesis of α-Amino-3-hydroxy-5-methyl-4-isoxazolepropionic Acid (AMPA) Receptor Subunit GluA1 by Carnitine Palmitoyltransferase 1C (CPT1C) in the Hippocampus*

Received for publication, July 30, 2015, and in revised form, September 2, 2015 Published, JBC Papers in Press, September 3, 2015, DOI 10.1074/jbc.M115.681064

Rut Fadó[‡], David Soto[§¶1], Alfredo J. Miñano-Molina[‖], Macarena Pozo[‡2], Patricia Carrasco[‡ ‡‡3], Natalia Yefimenko[§¶], José Rodríguez-Álvarez[‖**], and Núria Casals[‡ ‡‡4]**

From the [‡]Basic Sciences Department, Facultat de Medicina i Ciències de la Salut, Universitat Internacional de Catalunya, Sant Cugat del Vallès 08195, Spain, the [§]Laboratori de Neurobiologia, Institut d'Investigació Biomèdica de Bellvitge (IDIBELL), Feixa Llarga s/n 08907, L'Hospitalet de Llobregat 08907, Spain, the [¶]Department of Pathology and Experimental Therapeutics, Faculty of Medicine, Universitat de Barcelona, Feixa Llarga s/n 08907, L'Hospitalet de Llobregat 08907, Spain, the [‖]Institut de Neurociències and Departament de Bioquímica i Biologia Molecular, Universitat Autònoma de Barcelona, Cerdanyola del Vallès 08193, Spain, the [**]Centro de Investigación Biomédica en Red de Enfermedades Neurodegenerativas (CIBERNED), Madrid 28031, Spain, and the [‡‡]Centro de Investigación Biomédica en Red de Fisiopatología de la Obesidad y la Nutrición (CIBEROBN), 15706 Santiago de Compostela, Spain

Background: One interacting partner of the AMPA receptor (AMPAR) complex in the endoplasmic reticulum is carnitine palmitoyltransferase 1C (CPT1C).
Results: CPT1C regulates synaptic AMPAR levels and synaptic transmission by post-transcriptional regulation of GluA1 protein synthesis.
Conclusion: CPT1C is a new regulator of AMPAR translation efficiency.
Significance: CPT1C modulation could be a new tool to prevent AMPAR decline and learning deficits.

The regulation of AMPA-type receptor (AMPAR) abundance in the postsynaptic membrane is an important mechanism involved in learning and memory formation. Recent data suggest that one of the constituents of the AMPAR complex is carnitine palmitoyltransferase 1C (CPT1C), a brain-specific isoform located in the endoplasmic reticulum of neurons. Previous results had demonstrated that CPT1C deficiency disrupted spine maturation in hippocampal neurons and impaired spatial learning, but the role of CPT1C in AMPAR physiology had remained mostly unknown. In the present study, we show that CPT1C binds GluA1 and GluA2 and that the three proteins have the same expression profile during neuronal maturation. Moreover, in hippocampal neurons of CPT1C KO mice, AMPAR-mediated miniature excitatory postsynaptic currents and synaptic levels of AMPAR subunits GluA1 and GluA2 are significantly reduced. We show that AMPAR expression is dependent on CPT1C levels because total protein levels of GluA1 and GluA2 are decreased in CPT1C KO neurons and are increased in CPT1C-overexpressing neurons, whereas other synaptic proteins remain unaltered. Notably, mRNA levels of AMPARs remained unchanged in those cultures, indicating that CPT1C is post-transcriptionally involved. We demonstrate that CPT1C is directly involved in the *de novo* synthesis of GluA1 and not in protein degradation. Moreover, in CPT1C KO cultured neurons, GluA1 synthesis after chemical long term depression was clearly diminished, and brain-derived neurotrophic factor treatment was unable to phosphorylate the mammalian target of rapamycin (mTOR) and stimulate GluA1 protein synthesis. These data newly identify CPT1C as a regulator of AMPAR translation efficiency and therefore also synaptic function in the hippocampus.

Carnitine palmitoyltransferase 1 (CPT1)[5] is an enzyme classically involved in long-chain fatty acid transport across the

* This work was supported by Ministerio de Ciencia e Innovación (MICINN) Grants SAF2011-30520-C02-02 (to N. C.), SAF2011-30281 (to J. R.), and BFU2011-24725 (to D. S.) and Ministerio de Economía y Competitividad (MINECO) Grants SAF2014-52223-C2-2-R (to N. C.) and SAF2014-59697-R (to J. R.). This work was also supported by grants from CIBEROBN and CIBERNED (initiatives of ISCIII), the European Commission (FP7-PEOPLE-2011-CIG; Grant 293498 to D. S.), the Generalitat de Catalunya (Grants SGR2009-1231, SGR2009-152, SGR2014-0984, and SGR2014-465), and Fundació La Marató de TV3 Grant 2014-36-10 (to J. R.). The authors declare that they have no conflicts of interest with the contents of this article.
[1] Supported by the "Ramón y Cajal" Programme (RyC-2010-05970). Present address: Neurophysiology Laboratory, Dept. of Physiological Sciences I, Medical School, Universitat de Barcelona, Casanova 143, 08036 Barcelona, Spain.
[2] Recipient of a fellowship from the Agència de Gestió d'Ajuts Universitaris i de la Recerca (AGAUR) in Catalunya.
[3] Present address: Tumor Angiogenesis Group, Translational Research Laboratory, Institut d'Investigació Biomèdica de Bellvitge (IDIBELL), Feixa Llarga s/n 08907, L'Hospitalet de Llobregat 08907, Spain.
[4] To whom correspondence should be addressed: Basic Science Dept., Facultat de Medicina i Ciències de la Salut, Universitat Internacional de Catalunya, Josep Trueta s/n, Sant Cugat del Vallés 08195, Spain. Tel.: 34-935-042-002; Fax: 34-935-042-001; E-mail: ncasals@uic.es.

[5] The abbreviations used are: CPT1, carnitine palmitoyltransferase 1; AMPAR, AMPA-type receptor: chemLTD, chemical long term depression; DIV, days *in vitro*; ER, endoplasmic reticulum; mEPSC, miniature excitatory postsynaptic current; EV, empty vector; mTOR, mammalian target of rapamycin; PSD95, postsynaptic density protein 95; ANOVA, analysis of variance; BDNF, brain-derived neurotrophic factor; AMPK, 5′ AMP-activated protein kinase; GM1, monosialotetrahexosylganglioside.

mitochondrial intermembranes. Whereas liver CPT1A and muscle CPT1B isoforms catalyze the conversion of long-chain acyl-CoA to acyl-carnitines in fatty acid β-oxidation, the brain-specific isoform CPT1C exhibits low catalytic activity *in vitro* (1) and is located in the endoplasmic reticulum of neurons, largely in the hippocampus. Furthermore, it is exclusively present in mammals (1, 2).

The biochemical function of CPT1C is poorly understood, although it has been reported to modulate ceramide metabolism in neurons (3). At the physiological level, it is well demonstrated that hypothalamic CPT1C contributes to the control of food intake and energy balance (4–6) and the role of CPT1C in motor function (7, 8). Recently, the involvement of hippocampal CPT1C in cognition and spinogenesis has been described (3). CPT1C knock-out (KO) mice were shown to present strongly compromised spatial learning and disrupted dendritic spine morphology by increasing immature filopodia and decreasing mature spines. Interestingly, high-resolution proteomic analyses have revealed CPT1C as one of the constituents of the complex of α-amino-3-hydroxyl-5-methyl-4-isoxazole-propionate-type glutamate receptors (AMPARs) (9–11), and a recent study has described the involvement of CPT1C in GluA1 trafficking (12). However, given that CPT1C only interacts with AMPARs in the ER, the role of CPT1C in AMPAR synthesis has been scarcely examined.

In the present study, we show that CPT1C binds to endogenous GluA1 and GluA2 subunits and regulates their expression in mouse hippocampi and in cultured hippocampal neurons, which is crucial for AMPARs to reach the synapsis and for synaptic transmission. Furthermore, we reveal that this regulation is exerted post-transcriptionally, at the level of the *de novo* protein synthesis, without affecting protein degradation. Consequently, synaptic AMPARs are diminished in CPT1C KO hippocampal cultures, correlating with a reduction in the amplitude of AMPAR-mediated miniature excitatory postsynaptic currents (mEPSCs). These data may explain the previously described involvement of CPT1C in dendritic spinogenesis and learning.

Experimental Procedures

Materials—Anti-CPT1C antibody was developed in our laboratory (1). Anti-GluN2A, anti-biotin, anti-β-tubulin, and anti-calreticulin were obtained from Sigma; anti-GluA1, anti-GluA2, and anti-synapsin I were obtained from Merck Millipore. Anti-postsynaptic density protein 95 (PSD95), anti-stargazin, and anti-GFP were obtained from Abcam. Anti-phospho-PERK Thr-980, anti-EIF2 Ser-51, anti-EIF2, anti-ATF4, and anti-GADD34 were obtained from Santa Cruz Biotechnology. Phospho-Akt Ser-473, phospho-ERK1/2, phospho-mTOR Ser-3448, and phospho-5′ AMP-activated protein kinase α (phospho-AMPKα) Thr-172 were sourced from Cell Signaling, and anti-GAPDH was obtained from Ambion. L-Serine-D7 was obtained from CDN Isotypes. All other reagents were purchased from Sigma or Life Technologies, Inc., unless otherwise specified.

Animals—CPT1C knock-out mice were developed as described previously (3). After 8 back-crosses with C57BL/6J mice, littermate homozygous CPT1C KO and wild type (WT) mice were crossed separately to obtain a line for each genotype, which were used in the experiments. Hippocampi were obtained from adult male mice. All animal procedures met the guidelines in Spanish legislation (BOE 32/2007) and were approved of by the local ethics committee.

Neuronal Cultures—Primary hippocampal mouse neurons were prepared from embryonic day 16 WT or CPT1C KO embryos and cultured as described previously (13).

Electrophysiology—For recordings of cultured hippocampal neurons at 15–16 days *in vitro* (DIV), coverslips were mounted and placed on the stage of an inverted microscope (Olympus IX50). Whole-cell patch clamp currents were recorded with an Axopatch 200B amplifier-Digidata1440A series interface board using pClamp10 software (Molecular Devices). To isolate AMPAR-mediated mEPSCs, the following blockers were added to the extracellular solution: 1 μM tetrodotoxin, 50 μM D-AP5, 25 μM 7-CK, and 20 μM SR95531/gabazine (all from Abcam). Series resistance (R_s) was typically 15–22 megaohms and was monitored at the beginning and at the end of the experiment. Cells that showed a change in R_s greater than 20% were rejected (14). There was no significant difference in membrane capacitance when comparing WT and CPT1C KO neurons. For electrophysiology data analysis, mEPSCs were filtered at 5 kHz and digitized at 10 kHz. Data were analyzed using IGOR Pro (Wavemetrics) together with Neuromatic (Jason Rothman). Events were detected using amplitude threshold crossing (15), with the threshold (typically ~7–8 pA) set according to the baseline current variance. For amplitude and kinetic analyses, only events with monotonic fast rise (<1 ms) and uncontaminated decay were included.

Immunocytochemistry—For labeling surface AMPARs, neurons at 17–18 DIV were fixed with 4% (w/v) paraformaldehyde, blocked with 2% goat serum, and incubated with anti-AMPAR N terminus antibodies. After washing, cells were incubated with the appropriate Alexa Fluor-conjugated secondary antibodies. Neurons were then permeabilized with 0.1% (v/v) Triton X-100 and then blocked once more. Buffer was substituted with the appropriate anti-PSD95 antibody. After washing, cells were incubated with secondary antibodies. Coverslips were mounted using Fluoromount mounting medium. Imaging was performed with the confocal laser-scanning microscope ZEISS LSM 700 using a ×63 1.4 numerical aperture oil objective. For quantification, sets of cells were cultured and stained simultaneously and imaged using identical settings. The region of interest was randomly selected. Measurements with the Fiji image processing package were performed as described previously (16).

Immunoprecipitation—Neurons were collected using Triton buffer (50 mM Tris-HCl, pH 8, 150 mM NaCl, and 1% Triton X-100) supplemented with protease and phosphatase inhibitor cocktails and solubilized for 30 min at 4 °C in an orbital shaker. Samples were processed as described previously (17).

Western Blot—Dissected hippocampi and neuronal cultures were collected in radioimmune precipitation assay buffer and HEPES buffer (10 mM HEPES, 10 mM KCl, 1.5 mM $MgCl_2$), respectively, and supplemented with protease and phosphatase inhibitor mixtures. Next, protein extracts were separated on SDS-polyacrylamide gels and then transferred onto Immo-

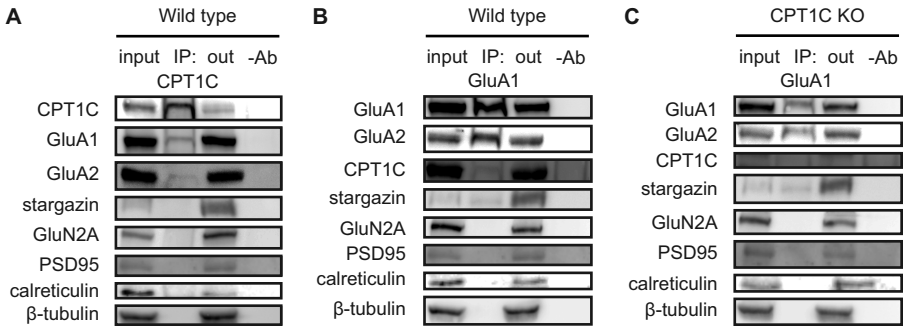

FIGURE 1. **CPT1C-GluA1-GluA2 endogenous interaction in hippocampal neurons.** CPT1C (*A*) or GluA1 (WT (*B*) or KO (*C*) neurons) was immunoprecipitated at 14 DIV, and proteins were detected by immunoblot in whole lysate (*input*), immunoprecipitated samples (*IP*), unbound samples (*out*), and samples cleaned with Protein G without an antibody (−*Ab*). Stargazin, GluN2A, PSD95, calreticulin, and tubulin were used as negative controls.

bilon-P PVDF membranes (Millipore). Blots were blocked with 5% (w/v) dry milk in TBS-T and incubated at 4 °C overnight with primary antibodies in TBS-T 0.2% (w/v) BSA. After washing, blots were incubated with horseradish peroxidase-conjugated secondary antibodies and developed using the Luminata™ Forte Western HRP substrate (Millipore). Semiquantitative analysis was performed using densitometry with Fiji software.

Lentiviral Infection—Two lentiviral vectors, pWPI-IRES-GFP and pWPI-CPT1C-IRES-GFP, were constructed to drive cell expression of GFP and CPT1C plus GFP, respectively. The map and the sequences of these plasmids, kindly provided by Dr. Trono (Laboratory of Virology and Genetics, Ecole Polytechnique Fédérale de Lausanne, Switzerland), are available from Addgene. Lentiviruses were propagated and titrated as described previously (18). Infection was performed on the day of seeding in complete DMEM medium at 1 virus/cell and left to stand for 5 h. The medium was then replaced with supplemented neurobasal medium. Fourteen days later, cells were collected for the analysis of GFP and CPT1C expression. The percentage of infected cells reached at least 75% in cultured hippocampal neurons.

Real-time PCR—For expression analysis, template cDNA was prepared from 1 μg of total RNA by reverse transcription (Moloney murine leukemia virus). Gene expression was quantified using real-time PCR with SsoFast Probes Supermix (Bio-Rad) and gene-specific primer VIC, FAN, or HEX dye-labeled as follows: *Gapdh* forward, reverse, and probe (4352339F; Applied Biosystems); *Gria1* (64845347; IDT); and *Gria2* (64845351; IDT) on a CFX96 real-time system (Bio-Rad). All biological samples were amplified in the same run for each experiment. Relative gene expression between paired samples was estimated using the $2^{-\Delta\Delta Ct}$ method.

Bio-orthogonal Noncanonical Amino Acid Tagging Analysis—The *de novo* protein synthesis rate was determined by a bio-orthogonal noncanonical amino acid tagging assay in WT or CPT1C KO hippocampal neurons as described previously (19), using copper sulfate and tris(2-carboxyethyl) phosphine to generate the Cu(I) catalyst for the copper-catalyzed azide-alkyne cycloaddition reaction (20). Briefly, cells were depleted of methionine for 30 min before treatment with azidohomoalanine at 1 mM (an effective surrogate for methionine; Jena Bioscience) for 4 h. After cell lysis with 0.05% SDS in PBS, pH 7.6, and protease and phosphatase inhibitors, the copper-catalyzed azide-alkyne cycloaddition reaction was prepared as follows: 200 μM triazole ligand, 50 μM biotin-alkyne, 400 μM tris(2-carboxyethyl) phosphine, and 200 μM copper sulfate, incubated at 4 °C overnight under agitation. The excess reagents were removed by gel filtration using PD-10 columns and eluted in 0.05% SDS in PBS, pH 7.6. A dot-blot analysis was performed to determine the newly synthesized protein concentration tagged with biotin. Desalted samples were precipitated with NeutrAvidin resin (Pierce) overnight at 4 °C. NeutrAvidin beads were then washed three times with 1% Nonidet P-40 in PBS, pH 7.6, and samples were eluted with SDS sample buffer. Proteins were detected using immunoblotting.

Statistics—Statistical analysis was performed using PRISM (GraphPad Software). Significance between two groups was determined according to data normality according to the Shapiro-Wilk test, using either Student's *t* test or a Mann-Whitney *U* test (parametric and non-parametric, respectively). For comparisons among 3–4 groups, ANOVA was performed, followed by the Bonferroni post-test.

Results

CPT1C-AMPAR Interaction in Hippocampal Neurons—It has been demonstrated that CPT1C binds AMPARs in solubilized membrane fractions from the hippocampus in rodents (9–11). We therefore first analyzed whether CPT1C was able to interact with AMPARs in cultured hippocampal neurons. We performed immunoprecipitation studies using specific anti-CPT1C antibodies developed in our laboratory (1). Fig. 1*A* shows how CPT1C interacts with GluA1 and GluA2 but not with other synaptic glutamatergic proteins, such as NMDA-type glutamate receptor subunit GluN2A or the AMPAR auxiliary subunit stargazin (also called TARPγ2; transmembrane AMPA regulatory protein). We also performed reverse immunoprecipitation using a GluA1 antibody and confirmed that interaction (Fig. 1*B*). It is worth noting that GluA1-GluA2 and GluA1-stargazin bindings were not found to be disrupted in the absence of CPT1C (Fig. 1*C*). To prove antibody specificity, CPT1C immunoprecipitation was performed in the hippocampi of CPT1C KO animals; in those samples, we did not detect CPT1C or GluA1 in immunoblotting (data not shown). These data demonstrate that CPT1C binds AMPARs in cultured hippocampal neurons.

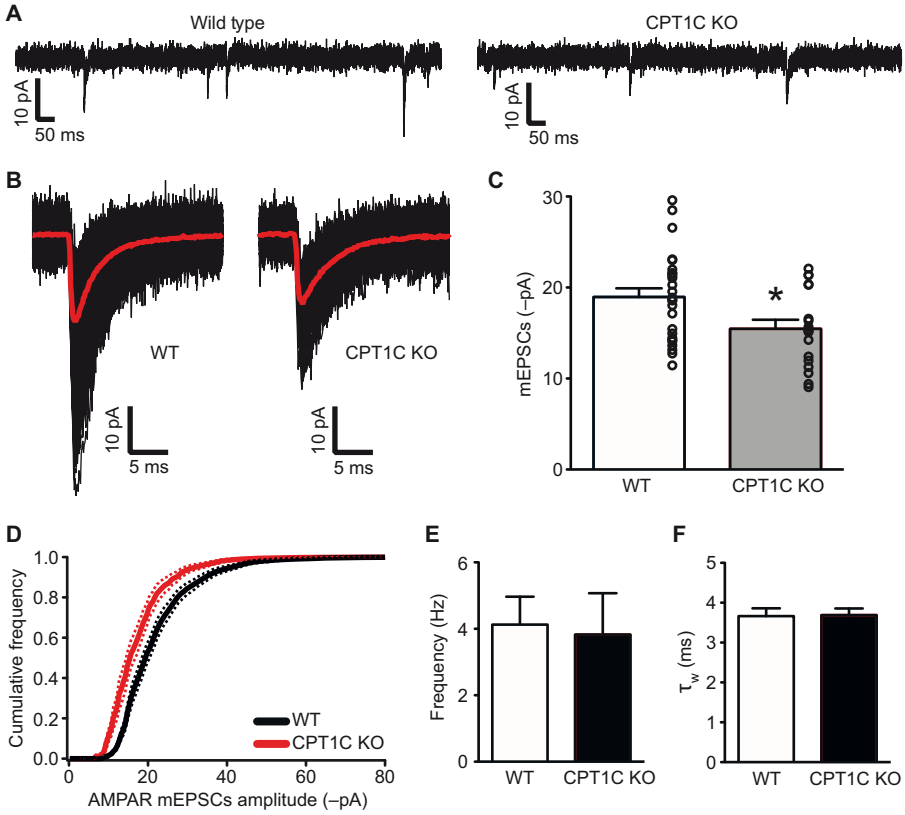

FIGURE 2. **mEPSC recordings in WT and CPT1C KO neurons.** *A*, representative whole-cell recordings from cultured hippocampal pyramidal neurons (15–16 DIV). Membrane potential was held at −60 mV. *B*, averaged mEPSCs (*red lines*) from recordings of two representative neurons. Individual mEPSCs are shown in *black*. *C*, individual average values for each single neuron superimposed on the bar graphs. *D*, cumulative probability distribution of mEPSC amplitude. *Continuous lines* represent average values. *Discontinuous lines* denote S.E. *E*, frequency of AMPAR miniature events. *F*, kinetics of the recorded AMPAR mEPSCs measured as the decay time constant with a double exponential (τ_w). *, $p < 0.05$. *Error bars*, S.E.

Synaptic Transmission Is Reduced in CPT1C KO Animals—Because CPT1C binds to GluA1/GluA2 and previous results from our laboratory clearly showed that spatial learning and dendritic spine maturation are impaired in CPT1C KO mice (3), we wondered whether excitatory synaptic transmission was altered in those animals. To address this issue, we performed whole-cell voltage clamp recordings of cultured hippocampal neurons and measured AMPAR-mediated mEPSCs. Cells were treated with tetrodotoxin to block synaptic transmission and with D-AP-5, 7-CK, and SR95531 to block NMDA and $GABA_A$ receptors. We found that mEPSC amplitude was decreased in neurons from CPT1C KO animals (Fig. 2, *A*–*C*) when compared with WT neurons (−18.96 ± 0.95 pA for WT *versus* −15.46 ± 0.99 pA for KO; $n = 26$ and $n = 18$, respectively; $p = 0.0175$; *t* test). Cumulative amplitude histograms for mEPSCs (Fig. 2*D*) revealed that the distribution of amplitudes in CPT1C KO neurons shifted toward smaller values, indicating a decrease in the quantity of postsynaptic AMPARs. We then examined the frequency of AMPA-mediated mEPSCs and found no significant differences (4.12 ± 0.84 Hz for WT *versus* 3.83 ± 1.24 Hz for KO; $p = 0.3519$; Mann-Whitney test; Fig. 2*E*), demonstrating that no presynaptic alteration is present in CPT1C KO cells.

Next, we measured the decay time constant of AMPAR-mediated mEPSCs in WT and KO animals and did not observe any change (3.67 ± 0.20 ms for WT *versus* 3.69 ± 0.16 ms for KO; $p = 0.9256$; *t* test; Fig. 2*F*), suggesting that no alteration in AMPAR subunit composition takes place in CPT1C-deficient neurons (21).

CPT1C Deficiency Reduces the Quantity of AMPARs at the Synaptic Level—The decrease in postsynaptic AMPARs in CPT1C KO neurons was further confirmed when we analyzed the presence of surface GluA1 and GluA2 at synaptic puncta by double immunocytochemistry with the postsynaptic marker postsynaptic density protein 95 (PSD95) in cultured hippocampal neurons (Fig. 3*A*). Quantitative image analysis showed that the percentage of postsynaptic puncta containing AMPARs was reduced in CPT1C KO neurons (39.3 ± 2.4% with GluA1 for WT *versus* 27.8 ± 1.8% for KO, $p = 0.0002$ (Fig. 3*B*); 49.0 ± 1.9% with GluA2 *versus* 28.0 ± 2.1%; $p < 0.0001$ (Fig. 3*C*); *t* test) and that the intensity of synaptic AMPARs was particularly decreased in CPT1C KO hippocampal neurons when compared with WT (1.00 ± 0.06 GluA1 intensity for WT *versus* 0.77 ± 0.03 for KO, $p = 0.0033$, $n = 79$ and 69, respectively (Fig. 3*D*); 1.00 ± 0.04 GluA2 intensity *versus* 0.61 ± 0.03, $p < 0.0001$, $n = 74$ (Fig. 2*E*); *t* test).

Interestingly, the number of PSD95 puncta per 10 μm was increased (11.85 ± 0.76 puncta for WT *versus* 16.71 ± 1.14 for KO; $n = 79$ and $n = 69$, respectively; $p = 0.0004$; *t* test; Fig. 3*F*), and the size of PSD95 puncta was decreased in CPT1C-deficient neurons (1.00 ± 0.08 *versus* 0.61 ± 0.03; $p < 0.0001$; *t* test; Fig. 3*G*).

In summary, our results demonstrate that the number of AMPARs in synaptic puncta is clearly reduced and that basal

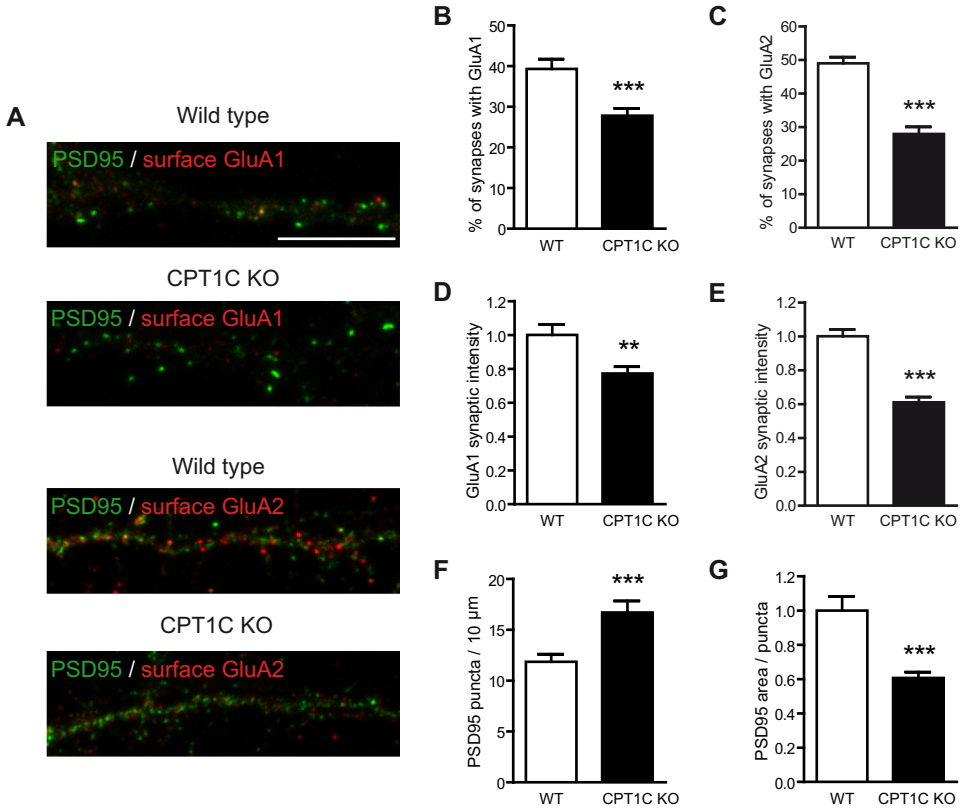

FIGURE 3. **Synaptic quantification of AMPARs in WT and CPT1C KO hippocampal neurons.** *A*, representative images of cultured hippocampal neurons at 17–18 DIV stained for surface GluA1 (*above*) or GluA2 (*below*) and PSD95. *Scale bar*, 10 μm. *B* and *C*, percentages of PSD95 puncta (synapses) containing AMPARs normalized to WT values. *D–E*, quantification of the intensity of synaptic AMPARs in positively stained PSD95 puncta. *F* and *G*, quantification of the number of PSD95 puncta/10 μm of dendrite length and the area of PSD95 puncta. All analyses were performed using 2 dendrites/neuron and 40 neurons/condition in two independent experiments performed in duplicate. Values shown as mean ± S.E. (*error bars*). **, $p < 0.01$; ***, $p < 0.001$.

synaptic activity is compromised in CPT1C KO animals. Based on these findings, we asked whether these deficits could be explained because CPT1C was involved in the regulation of AMPAR expression.

CPT1C Regulates AMPAR Protein Expression—AMPAR protein levels were first analyzed in hippocampal cultured neurons over DIV from 4 to 16 DIV. GluA1 and GluA2 expression intensified in the same manner as CPT1C during neuronal maturation (Fig. 4*A*). However, AMPAR levels in CPT1C KO cultured neurons were clearly diminished when compared with WT cells (1.00 ± 0.02 GluA1 levels for WT *versus* 0.45 ± 0.08 for KO at 14 DIV; $p = 0.0001$; and 1.00 ± 0.07 GluA2 levels *versus* 0.46 ± 0.10; $p = 0.0018$; $n = 5$; *t* test; Fig. 4*B*). Other synaptic proteins, including PSD95, synapsin I, and GluN2A, remained unaltered (not significantly different at 14 DIV; $n = 3$; *t* test; Fig. 4, *C* and *D*).

Previous results in our group demonstrated that the requirement of CPT1C for efficient spinogenesis is related with its ability to regulate ceramide levels; exogenous ceramide treatment rescues CPT1C KO phenotype on spine morphology. Therefore, we decided to analyze whether ceramide could reverse an AMPAR decrease in CPT1C-deficient neurons. Surprisingly, neither soluble C6 ceramide nor the treatment with the ceramide precursor serine increased GluA1 or GluA2 protein levels in KO cells (not significantly different; $n = 6$; *t* test; Fig. 4, *E–H*).

In contrast, exogenous CPT1C expression using lentiviral vectors rescued the decrease in GluA1 and GluA2 protein levels in CPT1C-deficient neurons without affecting GluN2A levels (Fig. 4*I*). Moreover, CPT1C overexpression in cultured WT hippocampal neurons was able to increase AMPAR protein levels (0.85 ± 0.40 GluA1 levels for empty vector (EV) *versus* 2.59 ± 0.48 for CPT1C; 0.82 ± 0.33 GluA2 levels for EV *versus* 2.64 ± 0.67 for CPT1C; $p < 0.05$; $n = 5$ for non-infected, $n = 3$ for EV, and $n = 5$ for CPT1C; ANOVA; Fig. 4*J*), demonstrating the capacity of CPT1C to enhance AMPAR expression.

Similar results were obtained in the hippocampi of CPT1C KO animals. First, we analyzed CPT1C expression during hippocampal development in WT mice. As seen in hippocampal cultures, total CPT1C protein levels were regulated with the same pattern expression as GluA1 and GluA2, which increases progressively up to adult age, as well as synapsin I, PSD95, and GluN2A (Fig. 5, *A* and *B*). To examine whether CPT1C was involved in the regulation of AMPAR expression, we measured total GluA1 and GluA2 protein levels in the hippocampi of adult CPT1C KO mice (Fig. 5*C*). CPT1C KO hippocampi showed lower levels of AMPARs when compared with WT mice (1.00 ± 0.04 GluA1 levels for WT *versus* 0.67 ± 0.07 for KO; $p = 0.0012$; 1.00 ± 0.05 GluA2 levels *versus* 0.67 ± 0.05; $p = 0.0002$; $n = 9$ for WT and $n = 13$ for KO; *t* test; Fig. 5*D*). PSD95, synapsin I, and GluN2A remained unaffected (not significantly different; $n = 6$; *t* test; Fig. 5, *E* and *F*). These findings

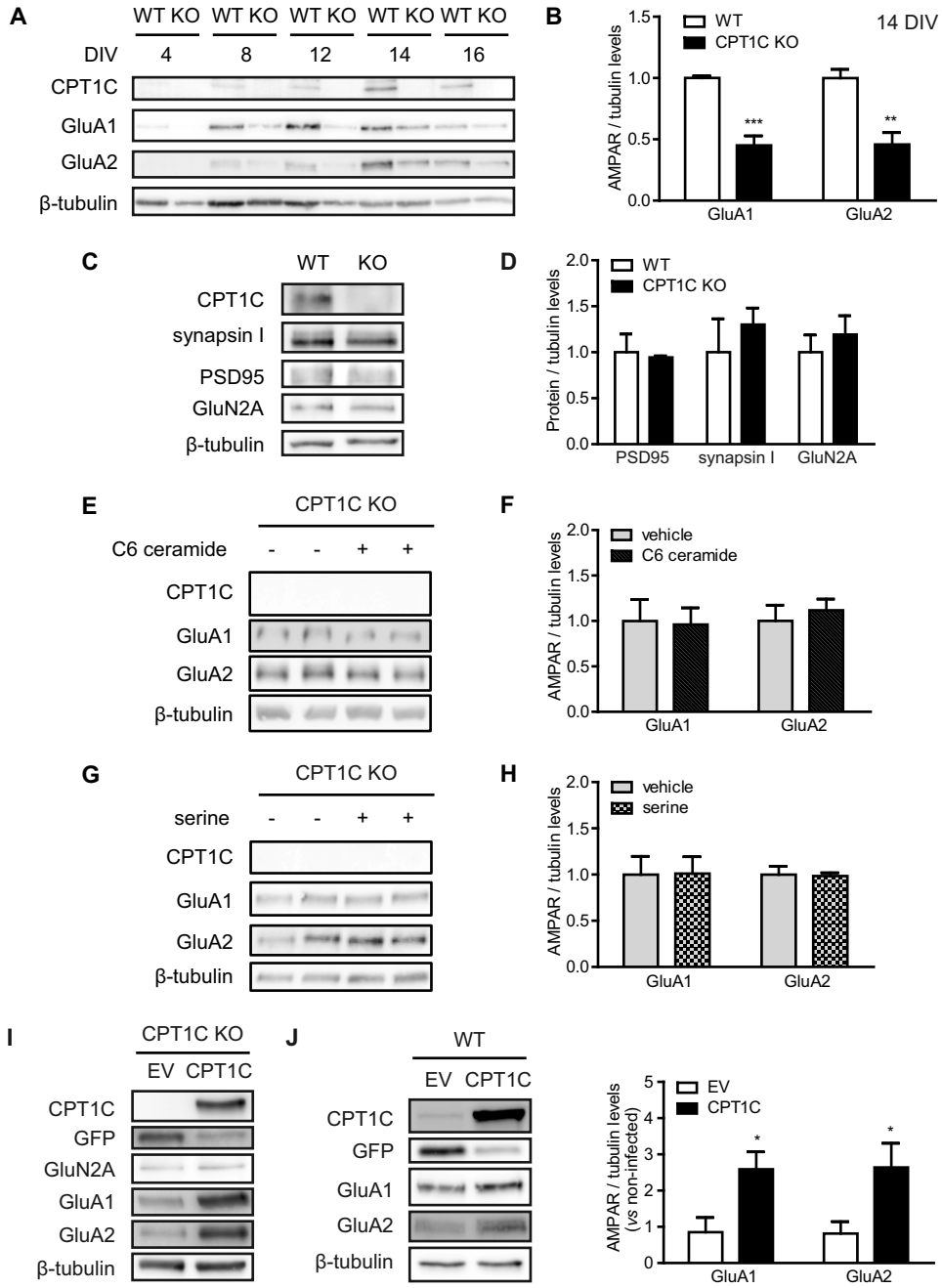

FIGURE 4. **CPT1C regulation of GluA1 and GluA2 expression in hippocampal neurons.** *A*, protein expression in hippocampal neurons from WT or CPT1C KO mice along the days *in vitro*. *B–D*, quantification of AMPARs and other synaptic proteins at 14 DIV. Tubulin was used as a loading control. Values are shown as mean ± S.E. (*error bars*) of 3–5 independent experiments. *E–H*, ceramide is unable to rescue AMPAR decrease in CPT1C KO neurons. Soluble C6-ceramide (1.5 μM) or vehicle (DMSO) was added to hippocampal neurons at 7 DIV. L-Serine-D7 (4 μM) was added at 13 DIV. Cells were collected at 14 DIV, and AMPAR levels were determined by immunoblotting. *I* and *J*, CPT1C-induced expression of AMPARs. Neurons obtained from CPT1C KO (*I*) and WT embryos (*J*) were infected with lentiviral CPT1C-IRES-GFP (CPT1C) or GFP alone (EV). At 14 DIV, protein levels were analyzed using immunoblotting. *, $p < 0.05$; **, $p < 0.01$; ***, $p < 0.001$.

confirm that CPT1C expression in the hippocampus specifically regulates total AMPAR protein levels.

CPT1C Regulates AMPAR Expression at the Post-transcriptional Level—In order to understand how CPT1C regulates AMPAR expression, we first analyzed *Cpt1c*, *Gria1*, and *Gria2* mRNA levels in WT and CPT1C KO mice during hippocampal development. Fig. 6*A* shows that *Cpt1c* mRNA levels increased during the first developmental days and then remained unaltered during the rest of the period of study (until 6 months of age). *Gria1* transcription exerted a similar pattern of expression than *Cpt1c* (Fig. 6*B*), whereas *Gria2* mRNA levels did not significantly change during hippocampal development (Fig. 6*C*). Interestingly, no differences were detected between WT and CPT1C KO animals in *Gria1* or *Gria2* mRNA levels ($n = 3–6$; *t* test; Fig. 6, *B* and *C*).

Moreover, hippocampal cultured neurons from CPT1C KO mice did not show any difference in mRNA levels when compared with WT neurons (not significantly different; $n = 6$; *t* test; Fig. 6*D*). In addition, CPT1C overexpression did not induce any change in the mRNA levels of either AMPAR (not significantly

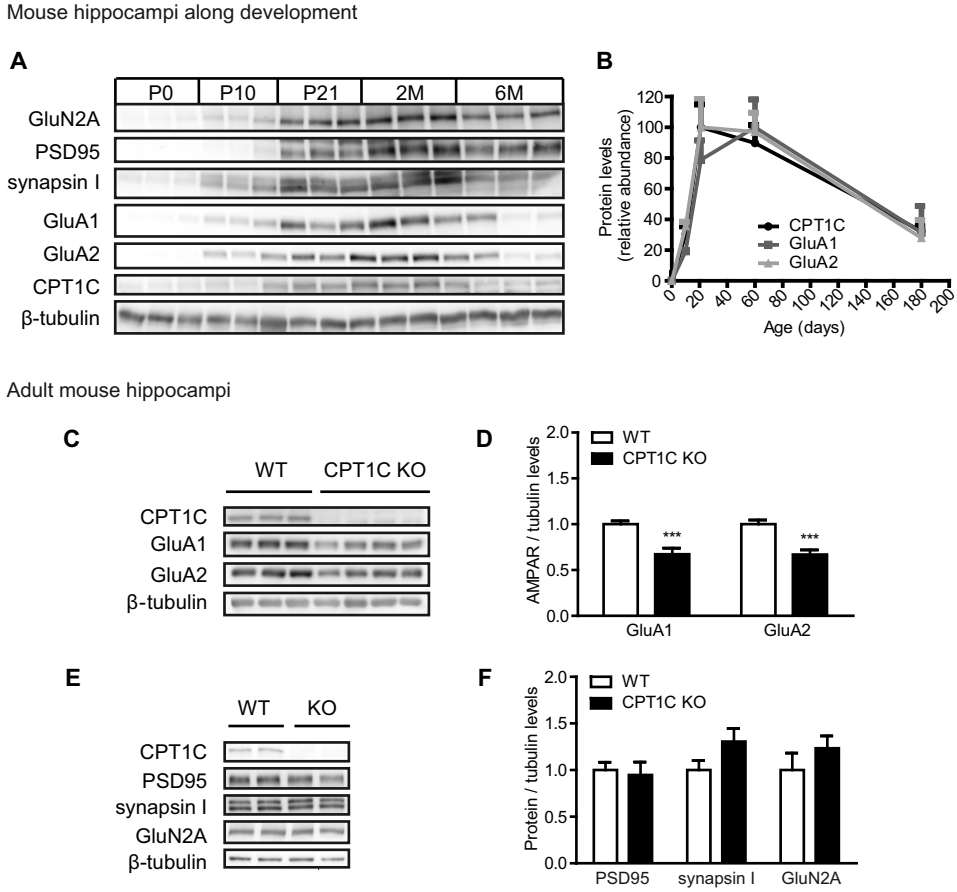

FIGURE 5. **GluA1 and GluA2 expression in the hippocampi of CPT1C KO animals.** *A* and *B*, Western blot analysis in whole lysates of hippocampi from C57BL/6J mice (*P*, postnatal day; *M*, month-old). Results were expressed as percentages of the most abundant levels over age ($n = 3$). *C–F*, protein levels in whole lysates of WT or KO adult mouse hippocampi (4 months of age; $n = 7$). ***, $p < 0.001$. *Error bars*, S.E.

different; $n = 6$; ANOVA; Fig. 6*E*). These data indicate that CPT1C does not regulate AMPARs at the transcriptional level and suggest that CPT1C is directly involved in protein turnover.

CPT1C Is Not Involved in AMPAR Degradation—The reduction in AMPAR protein levels observed in CPT1C-deficient neurons could be explained by enhanced degradation. To assay this possibility, we treated cells with a protein translation inhibitor, cycloheximide, and measured the decrease of AMPAR protein levels for 24 h. Results showed that GluA1 and GluA2 basal degradation was not enhanced in CPT1C KO neurons (not significantly different; $n = 3$; *t* test; Fig. 7*A*). In fact, there is a tendency in the opposite direction: a decrease in the rate of degradation, which may be due to the lower levels of synaptic AMPARs in those cells.

To further explore the degradation hypothesis, we analyzed whether activity-dependent GluA1 degradation was altered in CPT1C KO neurons. It is well described that chemical long term depression (chemLTD) triggers a persistent decrease in total GluA1 levels (22), a mechanism involving the proteasome (23). After NMDA treatment, the total levels of GluA1 decreased in both WT and CPT1C-deficient neurons (94.7 ± 1.5% in WT *versus* 73.1 ± 7.8% in KO; $n = 3$; not significantly different; *t* test; Fig. 7*B*), indicating that GluA1 degradation was not increased in CPT1C KO cells. Interestingly, CPT1C protein levels were also decreased in response to chemLTD (100.0 ± 12.5% for vehicle *versus* 50.8 ± 11.0% for NMDA in WT; $n = 3$; $p = 0.042$; *t* test; Fig. 7*C*), confirming the correlation between CPT1C and GluA1 expression.

CPT1C Regulates GluA1 Protein Synthesis—Because we did not observe significant differences at the level of transcription or degradation, we then explored whether CPT1C deficiency directly affected AMPAR protein synthesis. For this purpose, we measured GluA1 accumulation for 3 h after chemLTD by treating cultured neurons with inhibitors of proteasome and lysosome function to block protein degradation. We performed this analysis after chemLTD due to the very low AMPAR synthesis observed under basal conditions. As expected, an increase in GluA1 protein levels was detected in neurons from WT mice, whereas this increase was totally blocked in CPT1C KO neurons (145.2 ± 33.6% for WT *versus* 5.3 ± 11.9% for KO; $n = 3$; $p = 0.0171$; *t* test; Fig. 7*C*). Next, we used the bio-orthogonal noncanonical amino acid tagging method, which uses click chemistry to label methionine in newly synthesized proteins (see "Experimental Procedures" for a detailed description) to directly measure the *de novo* synthesis of GluA1 protein in both genotypes. WT or CPT1C KO hippocampal neurons were metabolically labeled with azidohomoalanine, and after conjugation to biotin, newly synthesized proteins were purified using NeutrAvidin beads. Immunoblotting of biotin-azidohomoalanine-labeled samples developed with NeutrAvidin showed similar total levels of the *de novo* synthetized proteins in both types

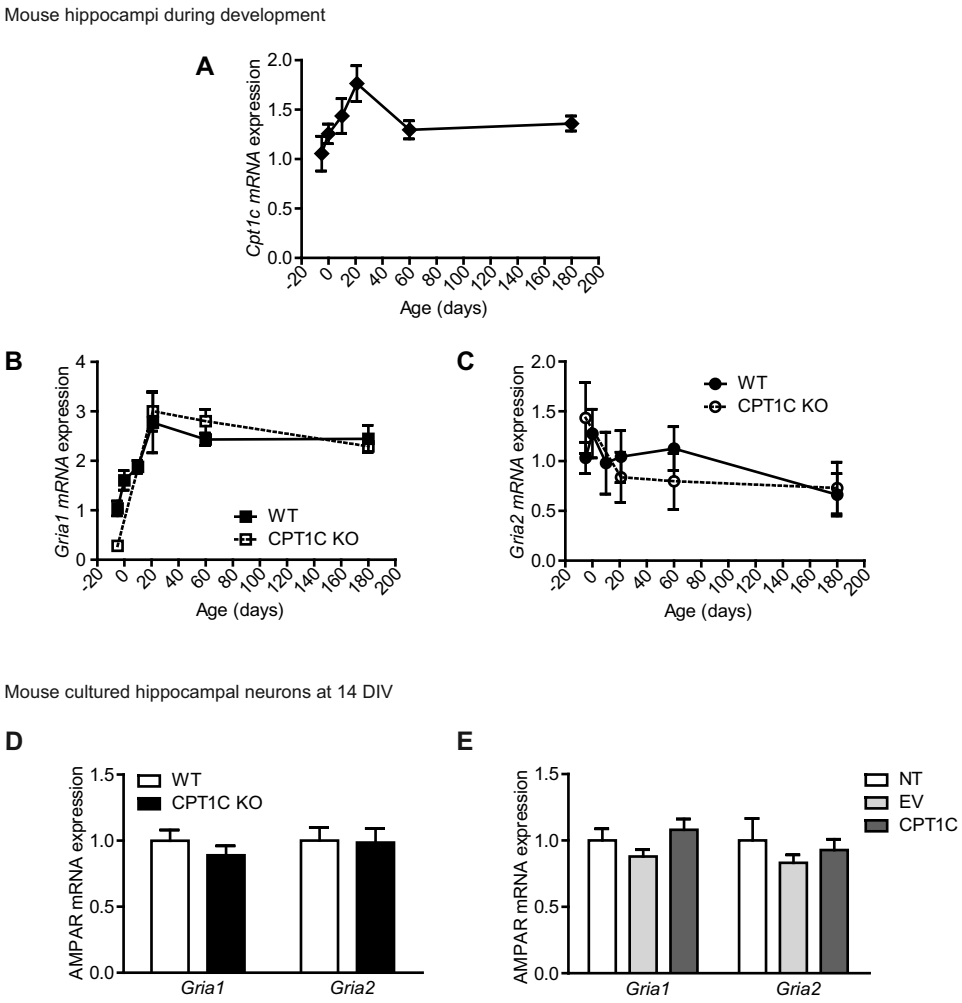

FIGURE 6. ***Gria1* and *Gria2* mRNA levels in CPT1C KO animals.** *A–C*, hippocampi were dissected from the following WT and CPT1C KO specimens: 17-day *post coitus* fetuses and 0-, 10-, 21-, 60-, and 120-day-old mice. *Cpt1c* (*A*), *Gria1* (*B*), and *Gria2* (*C*) mRNA levels were determined by real-time PCR. *Gapdh* was used as a housekeeping gene. Graphs show the mean ± S.E. (*error bars*) of 3 animals/group. *D*, AMPAR mRNA levels detected at 14 DIV in WT or CPT1C KO hippocampal neurons in culture. Results are shown as mean ± S.E. in three independent experiments performed in duplicate. *E*, *Gria1* and *Gria2* levels in WT neurons infected with lentiviral CPT1C. Results are shown as mean ± S.E. in two independent experiments performed in triplicate.

of cells (Fig. 7*D*, *left*). In contrast, the levels of newly translated (nascent) GluA1 protein in KO neurons were highly decreased compared with WT ones (Fig. 7*D*, *right*), indicating that the decrease observed in total levels of GluA1 comes from the reduction in protein synthesis. The voltage-dependent anion-selective channel, a mitochondrial protein not regulated by synaptic activity, did not show significant changes.

Because CPT1C is an ER protein, we wanted to determine whether the decrease in GluA1 synthesis was the result of a hypothetical ER stress response caused by CPT1C deficiency. For this purpose, we analyzed the levels of different effectors of the unfolded protein response pathway (24). We studied the levels of phospho-PERK (RNA-activated, protein kinase-like ER-resident kinase), phospho-EIF2 (eukaryotic initiation factor 2α), ATF4 (activating transcription factor 4), and GADD34 (a subunit of an EIF2-directed phosphatase) by immunoblotting; however, the unfolded protein response was not activated under basal conditions in CPT1C-deficient neurons (Fig. 7*E*).

CPT1C Is Required for Brain-derived Neurotrophic Factor (BDNF)-induced GluA1 Synthesis—It has been recently described that BDNF activates GluA1 translation through phosphorylation of mTOR (25). Therefore, we decided to explore whether CPT1C was necessary for BDNF-induced GluA1 synthesis. As expected, BDNF treatment was found to increase GluA1 protein levels in WT neurons; however, this increase was blocked in CPT1C KO cells (1.00 ± 0.03 for WT *versus* 1.30 ± 0.10 for WT with BDNF; $p < 0.05$; 0.60 ± 0.06 for KO *versus* 0.60 ± 0.06 for KO with BDNF; WT *versus* KO $p < 0.01$; WT with BDNF *versus* KO BDNF $p < 0.001$; $n = 8$; ANOVA; Fig. 8, *A* and *B*). Although Akt and ERK (well known BDNF downstream factors) were activated by the neurotrophin in both WT and KO neurons (for phospho-AKT: 1.00 ± 0.08 for WT *versus* 1.64 ± 0.11 for WT with BDNF; $p < 0.001$; 0.78 ± 0.08 for KO *versus* 1.34 ± 0.12 for KO with BDNF; $n = 8$; ANOVA (Fig. 8*C*); for phospho-ERK: 1.00 ± 0.09 for WT *versus* 4.78 ± 0.42 for WT with BDNF; $p < 0.001$; 0.73 ± 0.07 for KO *versus* 3.97 ± 0.40 for KO with BDNF; $n = 8$; ANOVA (Fig. 8*D*)), BDNF-induced mTOR phosphorylation was inhibited in KO cells (1.00 ± 0.15 for WT *versus* 1.61 ± 0.24 for WT with BDNF; $p < 0.05$; 0.98 ± 0.1 for KO *versus* 0.62 ± 0.17 for KO with BDNF; WT with BDNF *versus* KO BDNF $p < 0.01$; $n = 8$; ANOVA; Fig. 8*E*).

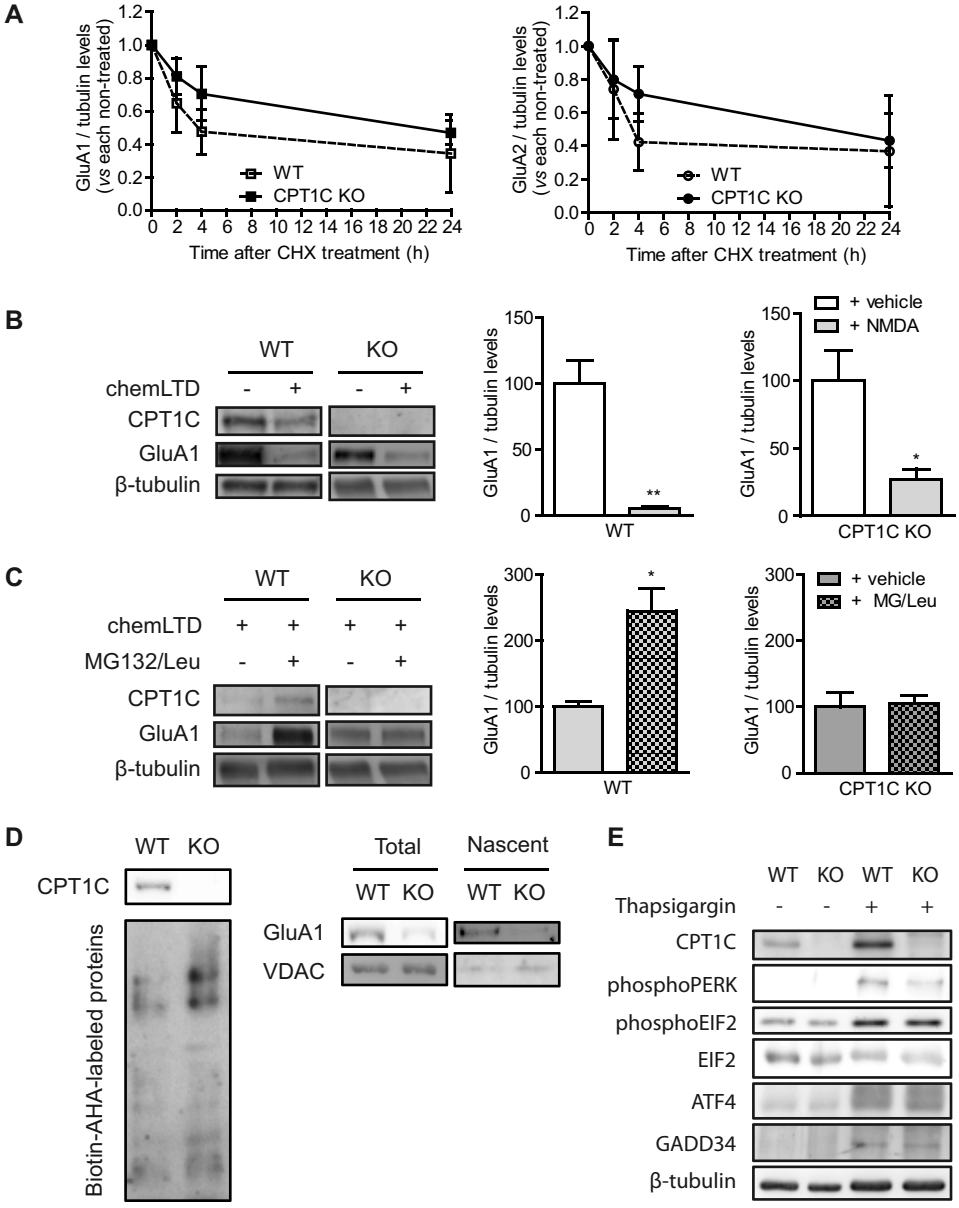

FIGURE 7. **CPT1C effects on AMPAR protein degradation and synthesis.** *A*, basal degradation of AMPARs. At 14 DIV, neurons were treated with cycloheximide (10 μM) for 24 h to inhibit protein translation. Protein levels were analyzed by immunoblot, and results were normalized to WT and CPT1C KO non-treated cells. Values are shown as the mean ± S.E. (*error bars*) in four independent experiments. *B*, NMDA-dependent degradation of GluA1. 14 DIV-cultured neurons were stimulated with NMDA (50 μM) for 5 min (chemLTD), and the medium was changed. Five hours later, cells were lysated, and protein levels were analyzed. *C*, GluA1 protein synthesis after chemLTD. Five hours after NMDA stimulation, neurons were treated with MG132 (10 μM) and leupeptin (200 μg/ml) for an additional 3 h. GluA1 accumulation was evaluated. The graphs show the values as mean ± S.E. in three independent experiments. *D*, *de novo* synthesis of GluA1. Total lysates (*left*) were obtained to analyze total biotin-azidohomoalanine-labeled proteins. GluA1 and voltage-dependent anion-selective channel (*VDAC*) (as control) were analyzed by immunoblotting in cell extracts (total) and in NeutrAvidin-bound fractions (nascent proteins; *right*). The image is representative of two independent experiments. *E*, analysis of endoplasmic reticulum stress markers in WT or CPT1C KO neuronal cultures. CPT1C, phospho-PERK, phospho-EIF2, ATF4, and GADD34 protein levels were determined by immunoblotting. Thapsigargin (ER stress inductor; 5 μM for 24 h) was used as a positive control. *, $p < 0.05$; **, $p < 0.01$.

Recently, it has also been described that phosphorylation of AMPK triggers GluA1 translation (26). Interestingly, CPT1C KO neurons show a reduction in the phosphorylation of this kinase under basal conditions (1.00 ± 0.07 for WT *versus* 0.41 ± 0.04 for KO; $n = 8$; $p < 0.001$; *t* test; Fig. 8, *F* and *G*). All of these data indicate that CPT1C is involved in GluA1 protein synthesis regulation under basal and stimulated conditions.

Discussion

In this study, we reveal that CPT1C regulates AMPAR protein levels by modulating its translational efficiency. CPT1C expression parallels GluA1 and GluA2 and other synaptic proteins during the development of the hippocampus and cultured hippocampal neurons. Moreover, CPT1C deficiency or CPT1C overexpression results in a specific decrease or increase, respectively, in total GluA1 and GluA2 levels without any change in their mRNA levels or degradation rate. The reduced expression of AMPARs results in reduced synaptic AMPAR content and diminished synaptic transmission in the hippocampal neurons of CPT1C KO mice, which may explain the impairment in dendritic spine maturation as well as the learning deficits we described previously in those mice (3).

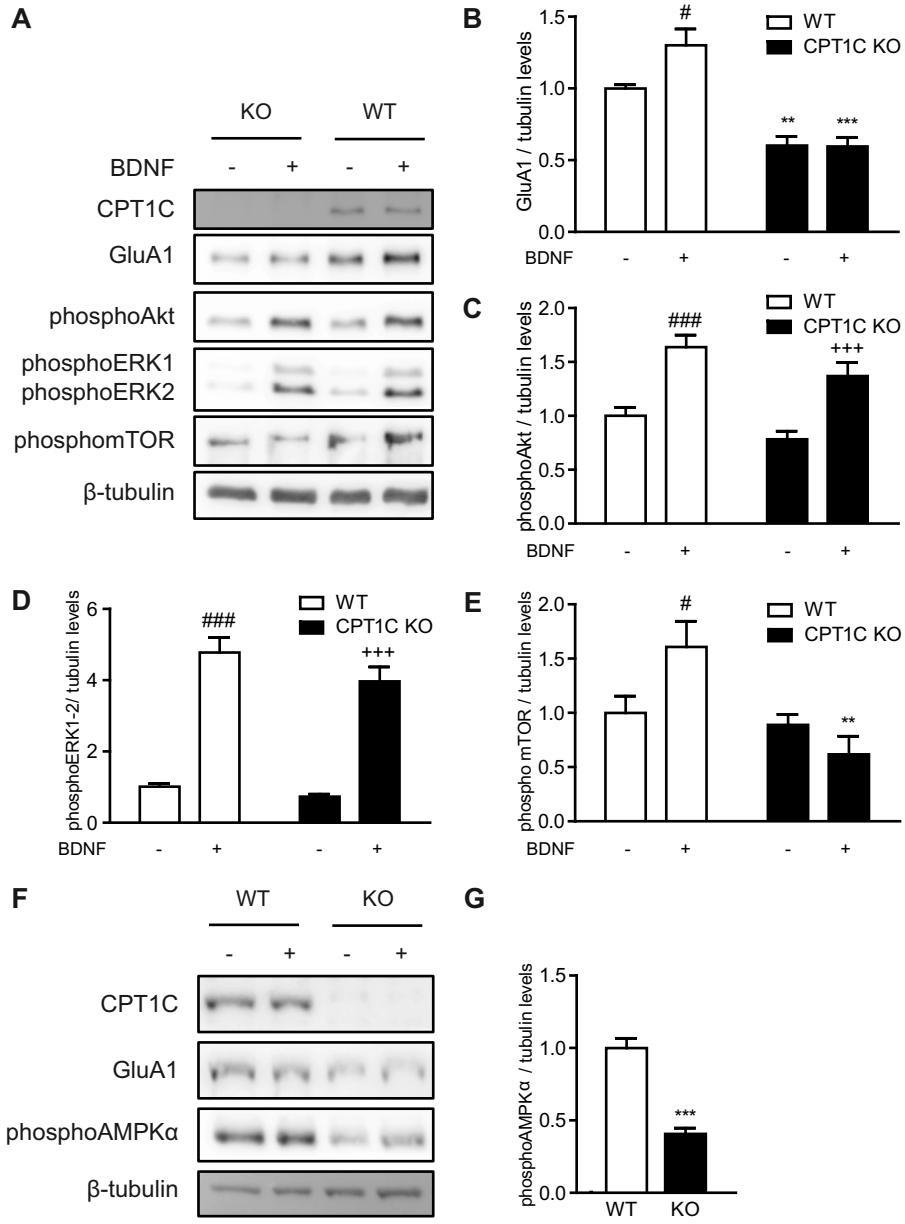

FIGURE 8. **BDNF-stimulated GluA1 synthesis is abolished in CPT1C KO neurons.** *A–E*, WT and KO hippocampal cultured neurons were treated at 14 DIV with BDNF (50 ng/ml for 1 h) to induce GluA1 synthesis. The protein levels of GluA1, phospho-Akt, phospho-ERK1/2, and phospho-mTOR were detected by immunoblotting. Tubulin was used as loading control. Results consist of the mean ± S.E. in two independent experiments performed in quadruplicate. *F* and *G*, AMPK activation in CPT1C KO hippocampal neurons. AMPKα phosphorylation was analyzed by Western blot (*WB*) in WT and CPT1C KO hippocampal neurons at 14 DIV. Tubulin was used as a loading control. Results are the mean ± S.E. (*error bars*) in two independent experiments performed in quadruplicate. *, $p < 0.05$; **, $p < 0.01$; ***, $p < 0.001$ KO *versus* WT in each condition; #, $p < 0.05$; ###, $p < 0.001$ WT non-treated *versus* WT BNDF; +++, $p < 0.001$ KO non-treated *versus* KO BDNF.

CPT1C Interaction with AMPARs—GluA1 and GluA2 were the first identified partners of CPT1C (9). The authors of that study demonstrated that CPT1C position within the macromolecular complex of AMPARs was more peripheral than other associated AMPAR constituents, but it appears to be one of the most abundant proteins of native AMPAR complexes in rodent brain solubilized membrane fractions. Unlike other AMPAR auxiliary proteins, CPT1C equally interacts with AMPARs in the hippocampus, cortex, and cerebellum (10), and CPT1C displays very similar richness profiles in AMPAR complexes across all brain regions (11). In the present study, we confirm the interaction of CPT1C with AMPARs in hippocampal neurons and show that CPT1C does not interact with other glutamate receptor constituents, such as GluN2A or stargazin. Interestingly, we observed a stronger interaction between CPT1C and GluA1 than between CPT1C and the GluA2 AMPAR subunit, suggesting that CPT1C has a greater influence on that subunit. Indeed, functional studies on expression systems have demonstrated that CPT1C enhances surface expression of homomeric GluA1 but has no effect on homomeric GluA2 (9), supporting the hypothesis of subunit specificity. The fact that CPT1C co-localizes with AMPARs only at the ER level and not at the Golgi apparatus or at the plasma membrane (12), together with the high abundance of CPT1C in hippocampal

AMPAR complexes, suggests that it could be involved in AMPAR synthesis or in AMPAR mobility and export from the ER to the surface, ultimately controlling AMPAR synaptic function. Recently, it has been demonstrated that CPT1C is involved in GluA1 trafficking (12). In the present study, we demonstrate that CPT1C is involved in GluA1 protein synthesis, confirming the role of CPT1C in both processes and indicating that CPT1C may be a key component in AMPAR homeostasis when located in the ER. It is important to note that biophysical gating properties of surface AMPARs (single channel conductance, peak open probability, and desensitization kinetics) are not modulated by CPT1C (12).

CPT1C Expression Profile—Interestingly, the CPT1C expression profile during hippocampal maturation after birth or during neuronal maturation in primary cultures resembled those of GluA1 and GluA2. In the hippocampus, the three proteins increased after birth, reaching their maximum values after weaning, and in hippocampal cultures, they also increased over DIV, the maximum taking place at 14 DIV. This expression profile, which is followed by other synaptic proteins, suggests that CPT1C function is closely related to synaptic function. In fact, activity-dependent degradation of AMPARs induced by chemLTD also coincides with a decrease in CPT1C protein levels, indicating a parallelism in CPT1C and AMPAR expression not only in terms of development but also in synaptic plasticity.

CPT1C Regulation of AMPAR Translation—Unlike other auxiliary proteins of the AMPAR complex that influence AMPAR trafficking, kinetics, and channel properties (27), CPT1C improves AMPAR translation efficiency. We show that the regulation of AMPAR expression by CPT1C is not exerted at the transcriptional level; nor is the basal degradation of AMPARs enhanced in KO CPT1C cells. By contrast, we clearly demonstrate that CPT1C regulates *de novo* synthesis of GluA1 under basal conditions using labeled methionine and that GluA1 synthesis after chemLTD is dependent on CPT1C availability. It would be interesting to study whether other synaptic stimulus, such as long term potentiation, which induces the delivery of AMPAR at the synaptic level, could regulate AMPAR synthesis mediated by CPT1C.

Few proteins have been previously related with AMPAR synthesis. It has been demonstrated that BDNF treatment of hippocampal neurons triggers GluA1 translation through phosphorylation of mTOR (28). The activation of mTOR blocks the translation repressor 4E-BP2, which selectively inhibits the synthesis of GluA1 in hippocampal pyramidal neurons, resulting in an increase of GluA1 protein translation (29). mTOR has been implicated in the regulation of dendritic growth (30, 31), spine formation (31–33), and synaptic function (32, 34). In the present study, we demonstrate that CPT1C KO neurons are unable to synthetize GluA1 in response to a BDNF stimulus; nor are they able to phosphorylate mTOR. It is unknown whether an activation of 4E-BP2 could explain the reduced expression of AMPARs in CPT1C-deficient neurons; however, our results suggest that CPT1C acts upstream from mTOR activation. CPT1C does not seem to regulate the PI3K/AKT pathway, because BDNF-induced phosphorylation of AKT at serine 473 is not impaired in CPT1C-deficient neurons. We are currently performing proteomic approaches to elucidate the mechanism by which CPT1C regulates GluA1 translation. The fact that we do not observe a complete loss of AMPARs in CPT1C KO neurons highlights the role of other mechanisms involved in AMPAR translation, such as the regulation of initiation and elongation by CPEB3 (35) or the control of expression by miRNA501-3p (36). Recently, it has been demonstrated that the activation of the energy sensor AMPK is involved in GluA1 translation (26). In our model, we observe a strong decrease in the phosphorylation of this kinase in CPT1C KO neurons. Interestingly, CPT1C has been previously associated with mTOR and AMPK in situations of energy homeostasis and metabolic stress (5, 6, 37–39). CPT1C might be a link between energetic metabolism and learning through the direct regulation of AMPAR synthesis. We speculate that CPT1C is a sensor of the energetic status of the neuron through its ability to bind malonyl-CoA (2), an intermediate in the fatty acid synthesis, whose cellular levels in hippocampus fluctuate during fasting and feeding (40). In fact, it has been described that the regulation of energy metabolism contributes to AMPAR synaptic incorporation (41), synaptic plasticity (42, 43), and memory processes (44).

Synaptic Function in CPT1C KO Mice—Our data from mEPSCs demonstrate that AMPAR synaptic transmission is reduced in CPT1C KO animals, although the specific subunit composition seems not to be altered. These data correlate perfectly with the reduced quantity of both GluA1 and GluA2 receptors we observed in synaptic puncta in CPT1C KO hippocampal neurons. We propose that the 25–40% reduction in synaptic AMPARs is mainly due to the 40–55% decrease in the total levels of GluA1 and GluA2, although we cannot rule out that other mechanisms, such as trafficking, are involved.

Interestingly, in CPT1C KO neurons, the number of PSD95 puncta increases, whereas the area of the PSD95 puncta and the quantity of AMPARs in synaptic puncta diminishes. These data suggest that the number of immature synapses is increased, whereas the number of functional synapses is decreased in CPT1C KO cells, which is in agreement with our previous observation of increased filopodia and reduced mature spines (3) in cultured hippocampal neurons. It is well known that filopodia contain fewer synaptic AMPARs than shorter regular spines (45). Therefore, reduced levels of synaptic AMPARs in CPT1C-deficient hippocampal neurons may contribute to the immature morphology of the dendritic spines.

We had previously demonstrated that the treatment of CPT1C KO neurons with exogenous ceramide increased spine maturation and reversed the KO phenotype (3). However, exogenous ceramide was not able to rescue the depletion of GluA1 and GluA2 levels observed in CPT1C KO cells. These results indicate that ceramide is not modulating AMPAR expression itself but might be necessary for other mechanisms in spinogenesis. In fact, other studies have described the involvement of GM1 ganglioside (a ceramide derivative) in the regulation of GluA2-containing AMPAR synaptic content by acting on endocytosis (46).

In summary, our results demonstrate that CPT1C is necessary for an efficient translation of AMPARs. In CPT1C-deficient neurons, total AMPAR levels are decreased, causing syn-

aptic transmission impairment and most likely the learning deficits observed in CPT1C KO mice. In contrast, CPT1C overexpression increases AMPAR synthesis. The rise in AMPAR levels may be not sufficient to increase synaptic activity (47); however, it probably ensures an adequate GluA1 and GluA2 reservoir and availability for synapsis requirements. Because AMPAR disruption is a major causative agent of synaptic dysfunction in neurodegenerative diseases and aging (27), we hypothesize that CPT1C modulation could constitute a new tool to prevent AMPAR decline and learning deficits during aging and in neurodegenerative disease.

Author Contributions—R. F. designed, performed, and analyzed all the experiments with the exception of the electrophysiological study reflected in Fig. 2, which was designed, performed, and analyzed by D. S. and N. Y. A. J. M. and J. R. provided technical assistance, contributed to the interpretation of data, and provided important intellectual content. M. P. designed and constructed vectors for overexpression and silencing CPT1C and contributed to the preparation of figures. P. C. contributed to the conception and design of the experiments. N. C. conceived and coordinated the study and wrote the paper. All authors reviewed the results and approved the final version of the manuscript.

Acknowledgments—We thank Marta Pérez for technical assistance and Dr. Carme Gallego (IBMB-CSIC) for help with bio-orthogonal noncanonical amino acid tagging assay analysis.

References

1. Sierra, A. Y., Gratacós, E., Carrasco, P., Clotet, J., Ureña, J., Serra, D., Asins, G., Hegardt, F. G., and Casals, N. (2008) CPT1c is localized in endoplasmic reticulum of neurons and has carnitine palmitoyltransferase activity. *J. Biol. Chem.* **283,** 6878–6885
2. Price, N., van der Leij, F., Jackson, V., Corstorphine, C., Thomson, R., Sorensen, A., and Zammit, V. (2002) A novel brain-expressed protein related to carnitine palmitoyltransferase I. *Genomics* **80,** 433–442
3. Carrasco, P., Sahún, I., McDonald, J., Ramírez, S., Jacas, J., Gratacós, E., Sierra, A. Y., Serra, D., Herrero, L., Acker-Palmer, A., Hegardt, F. G., Dierssen, M., and Casals, N. (2012) Ceramide levels regulated by carnitine palmitoyltransferase 1C control dendritic spine maturation and cognition. *J. Biol. Chem.* **287,** 21224–21232
4. Gao, X. F., Chen, W., Kong, X. P., Xu, A. M., Wang, Z. G., Sweeney, G., and Wu, D. (2009) Enhanced susceptibility of Cpt1c knockout mice to glucose intolerance induced by a high-fat diet involves elevated hepatic gluconeogenesis and decreased skeletal muscle glucose uptake. *Diabetologia* **52,** 912–920
5. Ramírez, S., Martins, L., Jacas, J., Carrasco, P., Pozo, M., Clotet, J., Serra, D., Hegardt, F. G., Diéguez, C., López, M., and Casals, N. (2013) Hypothalamic ceramide levels regulated by cpt1c mediate the orexigenic effect of ghrelin. *Diabetes* **62,** 2329–2337
6. Gao, S., Zhu, G., Gao, X., Wu, D., Carrasco, P., Casals, N., Hegardt, F. G., Moran, T. H., and Lopaschuk, G. D. (2011) Important roles of brain-specific carnitine palmitoyltransferase and ceramide metabolism in leptin hypothalamic control of feeding. *Proc. Natl. Acad. Sci. U.S.A.* **108,** 9691–9696
7. Carrasco, P., Jacas, J., Sahún, I., Muley, H., Ramírez, S., Puisac, B., Mezquita, P., Pié, J., Dierssen, M., and Casals, N. (2013) Carnitine palmitoyltransferase 1C deficiency causes motor impairment and hypoactivity. *Behav. Brain Res.* **256,** 291–297
8. Rinaldi, C., Schmidt, T., Situ, A. J., Johnson, J. O., Lee, P. R., Chen, K. L., Bott, L. C., Fadó, R., Harmison, G. H., Parodi, S., Grunseich, C., Renvoisé, B., Biesecker, L. G., De Michele, G., Santorelli, F. M., Filla, A., Stevanin, G., Dürr, A., Brice, A., Casals, N., Traynor, B. J., Blackstone, C., Ulmer, T. S., and Fischbeck, K. H. (2015) Mutation in CPT1C associated with pure autosomal dominant spastic paraplegia. *JAMA Neurol.* **72,** 561–570
9. Schwenk, J., Harmel, N., Brechet, A., Zolles, G., Berkefeld, H., Müller, C. S., Bildl, W., Baehrens, D., Hüber, B., Kulik, A., Klöcker, N., Schulte, U., and Fakler, B. (2012) High-resolution proteomics unravel architecture and molecular diversity of native AMPA receptor complexes. *Neuron* **74,** 621–633
10. Chen, N., Pandya, N. J., Koopmans, F., Castelo-Székelv, V., van der Schors, R. C., Smit, A. B., and Li, K. W. (2014) Interaction proteomics reveals brain region-specific AMPA receptor complexes. *J. Proteome Res.* **13,** 5695–5706
11. Schwenk, J., Baehrens, D., Haupt, A., Bildl, W., Boudkkazi, S., Roeper, J., Fakler, B., and Schulte, U. (2014) Regional diversity and developmental dynamics of the AMPA-receptor proteome in the mammalian brain. *Neuron* **84,** 41–54
12. Gratacòs-Batlle, E., Yefimenko, N., Cascos-García, H., and Soto, D. (2014) AMPAR interacting protein CPT1C enhances surface expression of GluA1-containing receptors. *Front. Cell Neurosci.* **8,** 469
13. Fadó, R., Moubarak, R. S., Miñano-Molina, A. J., Barneda-Zahonero, B., Valero, J., Saura, C. A., Moran, J., Comella, J. X., and Rodríguez-Álvarez, J. (2013) X-linked inhibitor of apoptosis protein negatively regulates neuronal differentiation through interaction with cRAF and Trk. *Sci. Rep.* **3,** 2397
14. Lissin, D. V., Carroll, R. C., Nicoll, R. A., Malenka, R. C., and von Zastrow, M. (1999) Rapid, activation-induced redistribution of ionotropic glutamate receptors in cultured hippocampal neurons. *J. Neurosci.* **19,** 1263–1272
15. Kudoh, S. N., and Taguchi, T. (2002) A simple exploratory algorithm for the accurate and fast detection of spontaneous synaptic events. *Biosens. Bioelectron.* **17,** 773–782
16. Aoto, J., Martinelli, D. C., Malenka, R. C., Tabuchi, K., and Südhof, T. C. (2013) Presynaptic neurexin-3 alternative splicing trans-synaptically controls postsynaptic AMPA receptor trafficking. *Cell* **154,** 75–88
17. Miñano-Molina, A. J., España, J., Martín, E., Barneda-Zahonero, B., Fadó, R., Solé, M., Trullás, R., Saura, C. A., and Rodríguez-Alvarez, J. (2011) Soluble oligomers of amyloid-β peptide disrupt membrane trafficking of α-amino-3-hydroxy-5-methylisoxazole-4-propionic acid receptor (AMPAR) contributing to early synapse dysfunction. *J. Biol. Chem.* **286,** 27311–27321
18. Naldini, L., Blömer, U., Gage, F. H., Trono, D., and Verma, I. M. (1996) Efficient transfer, integration, and sustained long-term expression of the transgene in adult rat brains injected with a lentiviral vector. *Proc. Natl. Acad. Sci. U.S.A.* **93,** 11382–11388
19. Dieterich, D. C., Lee, J. J., Link, a J., Graumann, J., Tirrell, D. A., and Schuman, E. M. (2007) Labeling, detection and identification of newly synthesized proteomes with bioorthogonal non-canonical amino-acid tagging. *Nat. Protoc.* **2,** 532–540
20. Pedraza, N., Ortiz, R., Cornadó, A., Llobet, A., Aldea, M., and Gallego, C. (2014) KIS, a kinase associated with microtubule regulators, enhances translation of AMPA receptors and stimulates dendritic spine remodeling. *J. Neurosci.* **34,** 13988–13997
21. Mosbacher, J., Schoepfer, R., Monyer, H., Burnashev, N., Seeburg, P. H., and Ruppersberg, J. P. (1994) A molecular determinant for submillisecond desensitization in glutamate receptors. *Science* **266,** 1059–1062
22. Shehata, M., Matsumura, H., Okubo-Suzuki, R., Ohkawa, N., and Inokuchi, K. (2012) Neuronal stimulation induces autophagy in hippocampal neurons that is involved in AMPA receptor degradation after chemical long-term depression. *J. Neurosci.* **32,** 10413–10422
23. Fernández-Monreal, M., Brown, T. C., Royo, M., and Esteban, J. A. (2012) The balance between receptor recycling and trafficking toward lysosomes determines synaptic strength during long-term depression. *J. Neurosci.* **32,** 13200–13205
24. Volmer, R., and Ron, D. (2015) Lipid-dependent regulation of the unfolded protein response. *Curr. Opin. Cell Biol.* **33,** 67–73
25. Fortin, D. A., Srivastava, T., Dwarakanath, D., Pierre, P., Nygaard, S., Derkach, V. A., and Soderling, T. R. (2012) Brain-derived neurotrophic factor activation of CaM-kinase kinase via transient receptor potential canonical channels induces the translation and synaptic incorporation of

GluA1-containing calcium-permeable AMPA receptors. *J. Neurosci.* **32,** 8127–8137
26. Wang, G., Amato, S., Gilbert, J., and Man, H.-Y. (2015) Resveratrol up-regulates AMPA receptor expression via AMP-activated protein kinase-mediated protein translation. *Neuropharmacology* **95,** 144–153
27. Henley, J. M., and Wilkinson, K. A. (2013) AMPA receptor trafficking and the mechanisms underlying synaptic plasticity and cognitive aging. *Dialogues Clin. Neurosci.* **15,** 11–27
28. Fortin, D. A., Srivastava, T., and Soderling, T. R. (2012) Structural modulation of dendritic spines during synaptic plasticity. *Neuroscientist* **18,** 326–341
29. Ran, I., Gkogkas, C. G., Vasuta, C., Tartas, M., Khoutorsky, A., Laplante, I., Parsyan, A., Nevarko, T., Sonenberg, N., and Lacaille, J.-C. (2013) Selective regulation of GluA subunit synthesis and AMPA receptor-mediated synaptic function and plasticity by the translation repressor 4E-BP2 in hippocampal pyramidal cells. *J. Neurosci.* **33,** 1872–1886
30. Jaworski, J., Spangler, S., Seeburg, D. P., Hoogenraad, C. C., and Sheng, M. (2005) Control of dendritic arborization by the phosphoinositide-3′-kinase-Akt-mammalian target of rapamycin pathway. *J. Neurosci.* **25,** 11300–11312
31. Kumar, V., Zhang, M.-X., Swank, M. W., Kunz, J., and Wu, G.-Y. (2005) Regulation of dendritic morphogenesis by Ras-PI3K-Akt-mTOR and Ras-MAPK signaling pathways. *J. Neurosci.* **25,** 11288–11299
32. Tavazoie, S. F., Alvarez, V. A., Ridenour, D. A., Kwiatkowski, D. J., and Sabatini, B. L. (2005) Regulation of neuronal morphology and function by the tumor suppressors Tsc1 and Tsc2. *Nat. Neurosci.* **8,** 1727–1734
33. Chen, N., and Napoli, J. L. (2008) All-*trans*-retinoic acid stimulates translation and induces spine formation in hippocampal neurons through a membrane-associated RARα. *FASEB J.* **22,** 236–245
34. Lee, C.-C., Huang, C.-C., and Hsu, K.-S. (2011) Insulin promotes dendritic spine and synapse formation by the PI3K/Akt/mTOR and Rac1 signaling pathways. *Neuropharmacology* **61,** 867–879
35. Pavlopoulos, E., Trifilieff, P., Chevaleyre, V., Fioriti, L., Zairis, S., Pagano, A., Malleret, G., and Kandel, E. R. (2011) Neuralized1 activates CPEB3: a function for nonproteolytic ubiquitin in synaptic plasticity and memory storage. *Cell* **147,** 1369–1383
36. Hu, Z., Zhao, J., Hu, T., Luo, Y., Zhu, J., and Li, Z. (2015) miR-501–3p mediates the activity-dependent regulation of the expression of AMPA receptor subunit GluA1. *J. Cell Biol.* **208,** 949–959
37. Wolfgang, M. J., Cha, S. H., Millington, D. S., Cline, G., Shulman, G. I., Suwa, A., Asaumi, M., Kurama, T., Shimokawa, T., and Lane, M. D. (2008) Brain-specific carnitine palmitoyl-transferase-1c: role in CNS fatty acid metabolism, food intake, and body weight. *J. Neurochem.* **105,** 1550–1559
38. Zaugg, K., Yao, Y., Reilly, P. T., Kannan, K., Kiarash, R., Mason, J., Huang, P., Sawyer, S. K., Fuerth, B., Faubert, B., Kalliomäki, T., Elia, A., Luo, X., Nadeem, V., Bungard, D., Yalavarthi, S., Growney, J. D., Wakeham, A., Moolani, Y., Silvester, J., Ten, A. Y., Bakker, W., Tsuchihara, K., Berger, S. L., Hill, R. P., Jones, R. G., Tsao, M., Robinson, M. O., Thompson, C. B., Pan, G., and Mak, T. W. (2011) Carnitine palmitoyltransferase 1C promotes cell survival and tumor growth under conditions of metabolic stress. *Genes Dev.* **25,** 1041–1051
39. Reilly, P. T., and Mak, T. W. (2012) Molecular pathways: tumor cells co-opt the brain-specific metabolism gene CPT1C to promote survival. *Clin. Cancer Res.* **18,** 5850–5855
40. Tokutake, Y., Onizawa, N., Katoh, H., Toyoda, A., and Chohnan, S. (2010) Coenzyme A and its thioester pools in fasted and fed rat tissues. *Biochem. Biophys. Res. Commun.* **402,** 158–162
41. Ribeiro, L. F., Catarino, T., Santos, S. D., Benoist, M., van Leeuwen, J. F., Esteban, J. A., and Carvalho, A. L. (2014) Ghrelin triggers the synaptic incorporation of AMPA receptors in the hippocampus. *Proc. Natl. Acad. Sci. U.S.A.* **111,** E149–E158
42. Shanley, L. J., Irving, A. J., and Harvey, J. (2001) Leptin enhances NMDA receptor function and modulates hippocampal synaptic plasticity. *J. Neurosci.* **21,** RC186
43. Chen, L., Xing, T., Wang, M., Miao, Y., Tang, M., Chen, J., Li, G., and Ruan, D.-Y. (2011) Local infusion of ghrelin enhanced hippocampal synaptic plasticity and spatial memory through activation of phosphoinositide 3-kinase in the dentate gyrus of adult rats. *Eur. J. Neurosci.* **33,** 266–275
44. Carlini, V. P., Monzón, M. E., Varas, M. M., Cragnolini, A. B., Schiöth, H. B., Scimonelli, T. N., and de Barioglio, S. R. (2002) Ghrelin increases anxiety-like behavior and memory retention in rats. *Biochem. Biophys. Res. Commun.* **299,** 739–743
45. Matsuzaki, M., Honkura, N., Ellis-Davies, G. C. R., and Kasai, H. (2004) Structural basis of long-term potentiation in single dendritic spines. *Nature* **429,** 761–766
46. Prendergast, J., Umanah, G. K. E., Yoo, S.-W., Lagerlöf, O., Motari, M. G., Cole, R. N., Huganir, R. L., Dawson, T. M., Dawson, V. L., and Schnaar, R. L. (2014) Ganglioside regulation of AMPA receptor trafficking. *J. Neurosci.* **34,** 13246–13258
47. Hayashi, Y., Shi, S. H., Esteban, J. A., Piccini, A., Poncer, J. C., and Malinow, R. (2000) Driving AMPA receptors into synapses by long term potentiation and CaMKII: requirement for GluR1 and PDZ domain interaction. *Science* **287,** 2262–2267

Neurobiology:

Novel Regulation of the Synthesis of α -Amino-3-hydroxy-5-methyl-4-isoxazolepropionic Acid (AMPA) Receptor Subunit GluA1 by Carnitine Palmitoyltransferase 1C (CPT1C) in the Hippocampus

Rut Fadó, David Soto, Alfredo J. Miñano-Molina, Macarena Pozo, Patricia Carrasco, Natalia Yefimenko, José Rodríguez-Álvarez and Núria Casals

J. Biol. Chem. 2015, 290:25548-25560.
doi: 10.1074/jbc.M115.681064 originally published online September 3, 2015